

Effect of MgTiO₃ Doping on Dielectric and Elasticity Properties of CaCu₃Ti₄O₁₂ (CCTO) Ceramics

R.Rajmi, A.K.Yahya, M.I.M.Yusof

Faculty of Applied Sciences, Universiti Teknologi MARA, Shah Alam, Selangor, Malaysia.

Abstract: Effects of MgTiO₃ addition on dielectric properties of CCTO ceramics were investigated. Dielectric measurements were performed for (1-x) CaCu₃Ti₄O₁₂ - xMgTiO₃ (x = 0-0.3) in the temperature and frequency range of 300-413K and 10² - 10⁶ Hz, respectively. Pure CCTO (x=0) showed decrease in dielectric constant from 25,382 (at 10² Hz) to 14,924 (at 10⁶ Hz) with increasing frequency. The dielectric loss of the sample decreased from 0.201 (at 10² Hz) to 0.140 (at 10⁶ Hz). Addition of MgTiO₃ caused reduction of dielectric constant with increasing x but significantly improved stability with frequency compared to the undoped x=0 sample. At x=0.1, reasonable values of the dielectric constant of 17,015 (at 10² Hz) and around 1.5-1.1 x10⁴ (at 10³ to 10⁶ Hz) was obtained. In addition, MgTiO₃ doping reduced the dielectric loss of the sample to around 0.15-0.10 in the range of 10⁴-10⁶ Hz. Further increase of MgTiO₃ at x=0.3 the dielectric loss was reduced to below 0.05 (at 10⁵ Hz). The reduction in dielectric loss could be attributed to the increase of grain boundary resistivity as the MgTiO₃ content increased and to the increase in grains boundary density as a result of smaller grains size. Dielectric constant versus temperature measurements showed increase in dielectric constant with increasing temperature for all samples. Activation energy obtained from Arrhenius plots of log of conductivity, s versus 1000/T showed considerable increase in grain-boundary activation energy, E_{gb}, with increasing MgTiO₃ content indicating possible increase in potential barrier as a result of the doping. On the other hand, addition of MgTiO₃ caused increase in shear and longitudinal velocity and related elastic moduli indicating improvement in elastic properties of CCTO with MgTiO₃ addition.

Key words: CCTO, Dielectric constant; dielectric loss; IBLC model; MgTiO₃

INTRODUCTION

Dielectric materials with high dielectric constant are widely used in microelectronic devices such as resonators, capacitors and others microelectronic devices where high dielectric constants allow smaller capacitive components, thus contributing to the decrease in size of electronic devices (Ramirez *et al.*, 2000; Subramaniam *et al.*, 2002). CaCu₃Ti₄O₁₂ (CCTO), a perovskite-related body-centered-cubic (bcc) compound has attracted much interest because of its high dielectric constant (Subramaniam *et al.*, 2000; Adams *et al.*, 2002). Previous reports (Subramaniam *et al.*, 2002; Capsoni *et al.*, 2004) showed that CCTO not only displayed weak variation of dielectric constant with frequency but also exhibits relatively small variation with temperature between 100 K and 400 K without undergoing any structural phase transition which makes it desirable for technological applications. This behavior of CCTO is in contrast with BaTiO₃ which has a large dielectric constant near its ferroelectric phase transition temperature (Mandal *et al.*, 2009). Nevertheless, one of the main problems for CCTO is the relatively high dielectric loss (tan δ) ≈ 0.1 at 1 kHz at room temperature which makes CCTO not attractive for practical applications (Subramaniam *et al.*, 2002; Feng *et al.*, 2006). So, decreasing the dielectric loss is a key point with the CCTO ceramic.

On the other hand, despite a number of studies that have been carried out, the origin of the intriguing dielectric phenomena of CCTO remains unclear. Some researches have suggested that the dielectric behavior involves intrinsic mechanisms (Chiodelli *et al.*, 2004) while others proposed mechanisms with extrinsic origins (Capsoni *et al.*, 2004; Mustafa *et al.*, 2009). Those who believe that the dielectric behavior of CCTO is not intrinsic in character argued that there is no structural phase transition in the whole temperature range to indicate any form of intrinsic mechanism. Thus many researchers tend to support the extrinsic mechanism

Corresponding Author: Mohd Isa Mohd Yusof, Faculty of Applied Sciences, UiTM, 40450 Shah Alam, Selangor, Malaysia.
E-mail: mohdi113@salam.uitm.edu.my

which is associated to crystalline deficiencies such as domain boundaries. One of the most acceptable explanations is the formation of barrier layers at the grain–grain boundary interfaces due to the slight loss of oxygen occurring during sintering as given by (Prakash *et al.*, 2008; Mandal *et al.*, 2009)



Equation (1) indicates that at sintering temperatures free electrons are released and this turns the material as n-type semiconductor. During cooling, reoxidation takes place and diffusion of oxygen gets more difficult as the grain boundaries are partially reoxidized. Therefore, oxygen diffusion is limited to grain boundaries which turn relatively more insulating compared to grains and lead to formation of barrier layers at grains–grain boundaries interfaces. Formation of the internal barrier layers was suggested to be the origin of the giant dielectric constant of CCTO. Based on the internal barrier layer capacitance, IBLC model, dielectric loss is closely related to insulation quality of the barrier layers as it increases with conductive leakage in the layers. Because higher resistance of the barrier layers will result in low conductance and improves dielectric loss, the dielectric loss in CCTO can be reduced efficiently by modification of grains boundaries with a view of increasing barrier layer resistance (Almeida *et al.*, 2004; Kang *et al.*, 2007).

Until now, a number of studies which attempted to reduce the dielectric loss while maintaining reasonable dielectric constant of the CCTO have been reported (Yueyue *et al.*, 2006; Sabar *et al.*, 2009). One approach was the use of elemental substitution such as Zr (Prakash *et al.*, 2008), and Nb (Sulaiman *et al.*, 2010) at Ti site and La (Feng *et al.*, 2006) at Ca site which were reported to reduce the dielectric loss in CCTO. The latter, for example, caused dielectric loss to reduce to 0.015 but suppressed the dielectric constant down to 3000. Other researchers reported effects of doping a secondary phase on CCTO e.g. Cr₂O₃-doped CCTO (Kwon *et al.*, 2007), SiO₂-doped CCTO (Kang *et al.*, 2007), GeO₂-doped CCTO (Amaral *et al.*, 2010) and Zn-doped CCTO (Sabar *et al.*, 2009). Others also have reported on CCTO doped with TiO₃-based composites such as CCTO–BaTiO₃ (Almeida *et al.*, 2004), CCTO–CaTiO₃ (Yueyue *et al.*, 2006) and CCTO–SrTiO₃ (Hongtao *et al.*, 2008). The latter showed low dielectric loss, $\tan \delta \approx 0.03$ while maintaining dielectric constant of slightly above 2000. In addition, Kwon *et al.*, 2007, reported improvement of dielectric constant and dielectric loss of doped of Cr₂O₃-doped CCTO to around 19,000 and $\tan \delta \approx 0.049$ respectively at 1 kHz at 1% Cr₂O₃. They suggested that the presence of the dopant at appropriate amounts resulted in the increase of grain boundary resistance which contributes to the low dielectric loss.

Quite recently, research done on addition of Magnesium Titanate (MT) to (Ba,Sr)TiO₃ (Lin *et al.*, 2005; Peng *et al.*, 2009) systems have resulted in significant improvement in reducing dielectric loss. The reduction in dielectric loss was suggested to be related to the decrease of grains size which affects grain boundary resistance. However, to the best of our knowledge, the effect of MgTiO₃ addition to the dielectric properties of CCTO has not been reported and it remains to be seen if addition of MT to CCTO could similarly modify its microstructure and grains boundaries which could lead to improvements in dielectric properties of CCTO. Besides that, the hardness and strength of the material's inter-atomic bonding are equally important. Since there are very limited studies on ultrasonic velocity measurements for titanate ceramics especially on CCTO ceramics, therefore it is also interesting to further investigate the effect of MgTiO₃ addition on the elastic properties of CCTO ceramics at room temperature.

In this work, polycrystalline (1-x) CaCu₃Ti₄O₁₂ – xMgTiO₃ (x=0-0.3) ceramics were synthesized using conventional solid-state synthesis method to investigate its dielectric properties in the temperature and frequency range of 300-413K and 10²–10⁶ Hz, respectively. The effects of MgTiO₃ addition to CCTO on both grains-boundary activation energy, E_{gb} and grain activation energy E_g will be discussed. In addition, results of longitudinal and shear ultrasonic velocity at room temperature of (1-x) CaCu₃Ti₄O₁₂ – xMgTiO₃ (x=0-0.3) will be also reported.

Experimental Details:

(1-x) CaCu₃Ti₄O₁₂ – xMgTiO₃ (x=0, 0.1, 0.2 and 0.3) ceramics were prepared by using solid state reaction technique from high purity chemicals (>99.99%) of calcium carbonate, (CaCO₃), titanium dioxide (TiO₂), copper oxide (CuO) and magnesium titanate (MgTiO₃). In the first stage, undoped CCTO were prepared by mixing and grinding the chemicals according to the stoichiometric ratio. The powder was then calcined at 950°C for 12 hours before reground and pressed as cylindrical pellets which were then sintered at 1050°C for 24 hours. Then, the sintered CCTO pellets were reground and mixed with MgTiO₃ according to stoichiometric ratios. The mixed powders were then ground and pressed into pellets which were sintered at 1050°C for 3 hours.

The crystalline phases of the prepared samples were investigated by XRD using Philips X'pert Pro model PW3040 diffractometer equipped with Cu-K_α radiation. The microstructures of the ceramics were recorded using LEO model 982 Gemini, scanning electron microscope (SEM).

The pellets were polished using fine sand paper to produce parallel opposite faces for ultrasonic velocity measurement. Ultrasonic velocity measurements at room temperature were measured in both longitudinal and shear modes at 5 MHz by applying the pulse-echo- overlap technique using Matec model 7700 system.

Impedance of samples was measured using a HIOKI 3531-Z Bridge interfaced to a computer in the frequency range of 10² Hz to 10⁶ Hz. The pellets were coated with aluminum foil and the dielectric properties were measured as a function of frequency in the temperature range 300 -413K. The plot of imaginary impedance, Z_i versus real impedance, Z_r were obtained in order to get grain resistance, R_g and grain boundary resistance, R_{gb}.

The real part of complex permittivity, ε_r and the imaginary part, ε_i is given by (Prakash *et al.*, 2008; Majid *et al.*, 2007):

$$\epsilon_r = \frac{Z_i}{\omega C_o (Z_r^2 + Z_i^2)} \quad (2)$$

$$\epsilon_i = \frac{Z_i}{\omega C_o (Z_r^2 + Z_i^2)} \quad (3)$$

Dissipative loss or dielectric loss, tan δ is given by:

$$\tan \delta = \frac{\epsilon_i}{\epsilon_r} \quad (4)$$

RESULTS AND DISCUSSION

Figure 1 shows the X-ray diffraction patterns for all samples. The undoped CCTO sample (x=0) was single phased with cubic perovskite structure with *Im3* space group. However, for x>0, in addition to the CCTO phase, peaks assigned to MgTiO₃ secondary phase were observed in addition to minute amounts of unidentified impurity peaks. The CCTO lattice parameters of all samples were a=7.4090(3) Å in very close agreement that reported in Ref. (Sung *et al.*, 2005). The constancy of the lattice parameter indicates that MgTiO₃ did not substitute into the CCTO structure. In addition, figure 1 show that intensity of MgTiO₃ related XRD peaks increases with MgTiO₃ contents, which confirms increasing percentage volume of MgTiO₃ phase. The density of samples (Table 1) decreased with MgTiO₃ addition. The decrease in density (ρ) of the samples with MgTiO₃ addition is probably due to the partial replacement of higher density CCTO (5.07 g/cm³) (Marques *et al.*, 2007) with lower density MgTiO₃ (3.62 g/cm³) (Cheng *et al.*).

Fig. 2 shows the scanning electron micrographs of undoped CCTO and MgTiO₃-doped CCTO samples. As observed, the average grain size, t_g of MgTiO₃-doped CCTO ceramics decreases significantly as compared to the undoped sample. Dielectric property is related to the microstructure as the effective permittivity can be calculated by using the expression, e_r α t_g/t_{gb}, where t_g and t_{gb} are the average grain size and thickness of the grain-boundary regions, respectively (Amaral *et al.*, 2010; Zang *et al.*, 2005). So, the decrease in grains size is expected to contribute to reduction of dielectric constant of the doped CCTO samples.

On the other hand, the effective dielectric constant of the CCTO-MgTiO₃ composites can be computed by using the Lichtenecker's logarithmic law (Sung *et al.* 2005; Hongtao *et al.*, 2008) given by the equation:

$$\ln \epsilon_{cal} = (1-x) \ln \epsilon_{CCTO} + x \ln \epsilon_{MT} \quad (5)$$

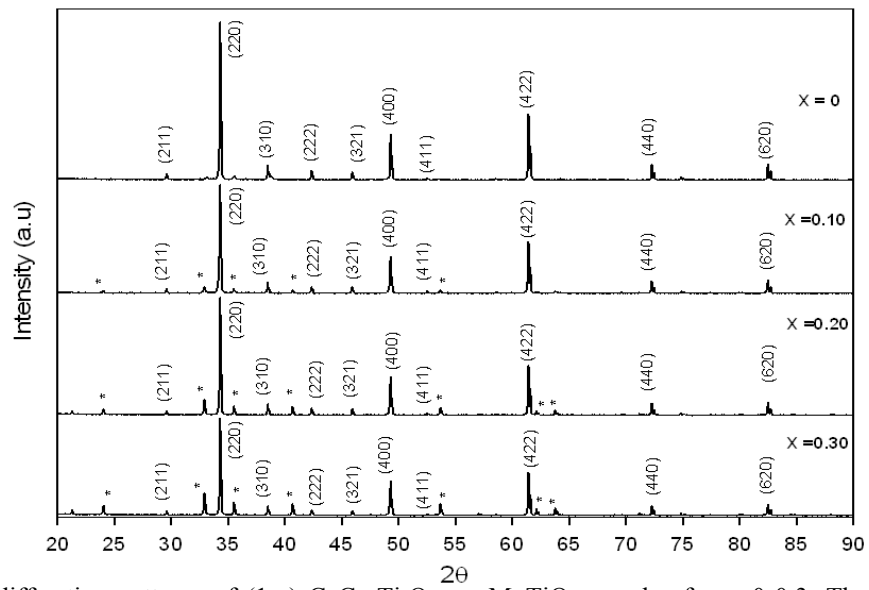
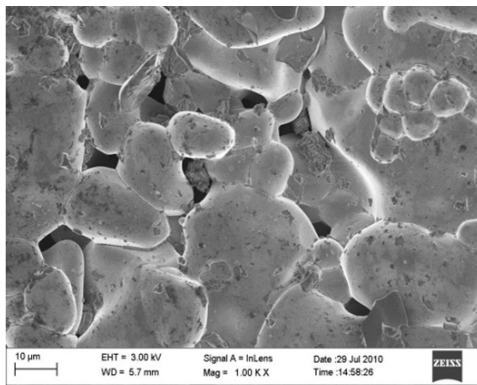
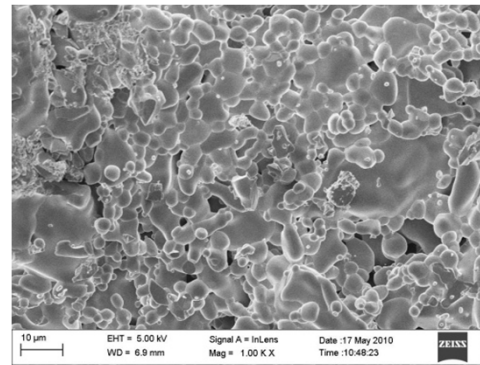


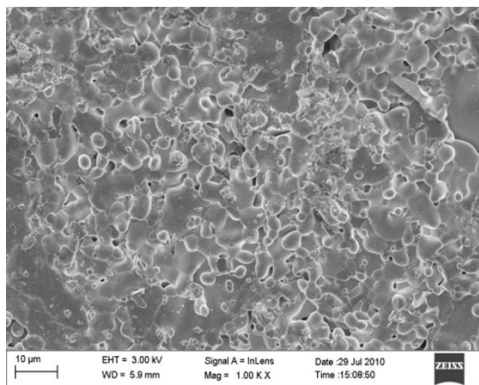
Fig. 1: X-ray diffraction patterns of $(1-x) \text{CaCu}_3\text{Ti}_4\text{O}_{12} - x\text{MgTiO}_3$ samples for $x=0-0.3$. The MgTiO_3 phase is indicated by (*).



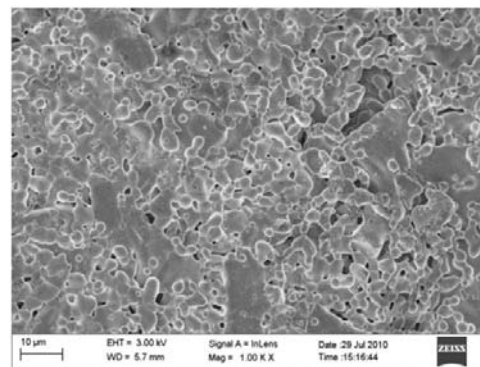
(a)



(b)



(c)



(d)

Fig. 2: SEM micrograph of internal sections of (a) $x = 0$ (b) $x = 0.10$ (c) $x = 0.20$ (d) $x = 0.30$ $(1-x) \text{CaCu}_3\text{Ti}_4\text{O}_{12} - x\text{MgTiO}_3$ samples.

where ϵ_{cal} , ϵ_{CCTO} and ϵ_{MT} represent the dielectric constant values of calculated CCTO, measured CCTO and $MgTiO_3$, respectively and x is the volume fraction of $MgTiO_3$ doping on CCTO. In this work, ϵ_{MT} is chosen as 21 from previous report (Lin *et al.*, 2005) and the experimental dielectric constant of the pure CCTO ceramics at room temperature and 1 KHz was 20,825. The calculated and measured dielectric constant values are plotted in Figure 3. The graph suggests that the measured values of dielectric constant are in slight agreement with the effective dielectric constant calculated using the Lichtenecker's logarithmic law. The disagreement between experimental and expected values could be due to the big difference between the dielectric constant of the two compounds that is the dielectric constants of dopant ($MgTiO_3$) and parent (CCTO) when applying the Lichtenecker's logarithmic law (Hongtao *et al.*, 2008). However, even though the Lichtenecker's logarithmic law could not predict accurately the effective dielectric constant of the CCTO mixture in such a case, the equation is useful in predicting the decreasing trend of the dielectric constant of the doped CCTO samples (Figure 3). In addition, the decrease in grains size as a result of doping (Figure 2), as mentioned above, may also be a contributing factor to the lower values of the measured dielectric constant compared to the calculated values.

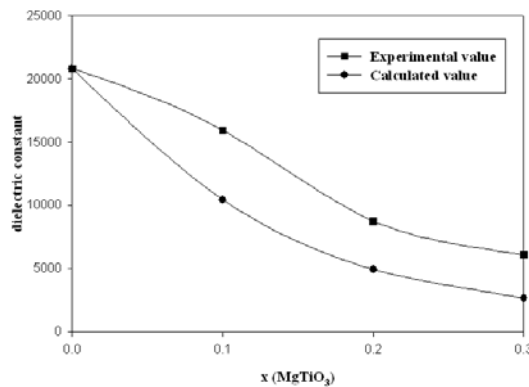


Fig. 3: The measured and calculated dielectric constant of $(1-x) CaCu_3Ti_4O_{12} - xMgTiO_3$ for $x=0-0.3$ at room temperature and 1 KHz.

CCTO ceramics, according to the IBLC model, consist of semiconducting grains and insulating grain boundaries. The effective method to confirm this is by using impedance spectroscopy (IS) ((Sung *et al.*, 2005; Feng *et al.*, 2006). The values of the grains resistance, R_g and the grain boundaries resistance, R_{gb} are obtained from the high frequency and low frequency intercepts, respectively of the semi-circles on the real impedance axis, Z_r (Subramaniam *et al.*, 2000; Capsoni *et al.*, 2004). At low frequencies, even though, charge carriers can move a larger distance, their movement gets limited due to potential barriers at the grain boundaries (Prakash *et al.*, 2008). The IS results derived from figure 4 show that the grain boundaries resistance, R_{gb} of the samples increases largely as x increases from 0 to 0.30 (Table 1). In contrast, at high frequencies, the charge carriers can move only in shorter distances within the grains without being affected by the grain boundaries. The grain resistance, R_g value derived from figure 4 changes little with x (Table 1). It is also interesting to note that values of ρ_{gb} are higher than the corresponding ρ_g values by four orders of magnitude which conform to the IBLC model.

Table 1: Density, ρ , Grains resistivity, ρ_g , grains boundary resistivity, ρ_{gb} , grains conductivity, s_g and grains boundary conductivity, s_{gb} at room temperature of all samples obtained from IS measurements

Samples (x)	$\rho(kgm^{-3})$	$\rho_g(\Omega.cm) \times 10^2$	$s_g(1/\Omega.cm) \times 10^{-3}$	$\rho_{gb}(\Omega.cm) \times 10^6$	$s_{gb}(1/\Omega.cm) \times 10^{-7}$
0	4840(2)	3.47	2.88	2.02	4.96
0.1	4808(2)	3.99	2.51	2.71	3.69
0.2	4630(1)	4.88	2.05	3.66	2.73
0.3	4376(2)	5.79	1.73	4.26	2.35

The dielectric constant of $(1-x) CaCu_3Ti_4O_{12} - xMgTiO_3$ for $x = 0-0.3$ measured at room temperature over the frequency range of $10^2 \sim 10^6$ Hz were plotted in Fig.5. The dielectric constant of undoped $x = 0$ sample dropped from 25,382 (at 10^2 Hz) to 14,924 (at 10^6 Hz), as the frequency increases. The decrease in dielectric constant with frequency could be due to several polarization mechanisms (Sabar *et al.*, 2009; Wang *et al.*, 2010). However the relaxation times of space charge and dipolar polarizations generally participate only at

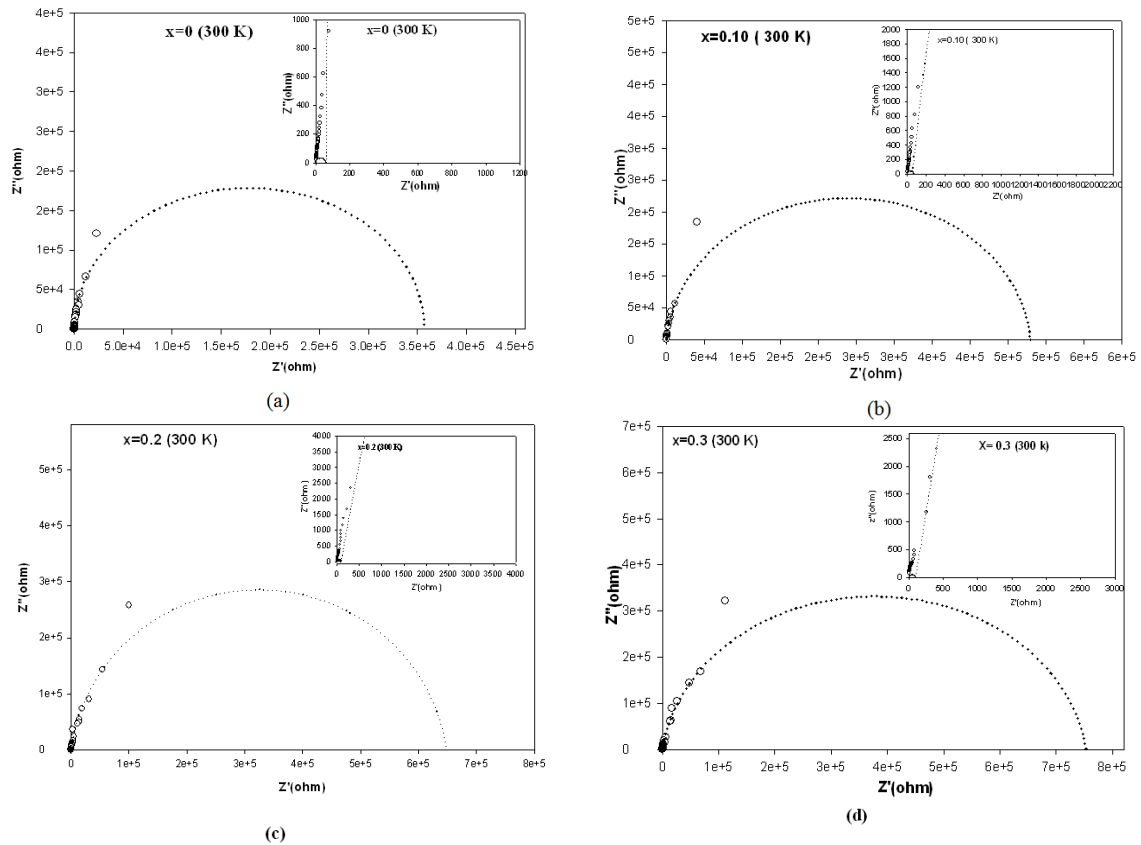


Fig. 4: The complex plane impedance (Z'' versus Z') plots of (a) $x = 0$ (b) $x = 0.10$ (c) $x=0.20$ (d) $x=0.30$, $(1-x)$ $\text{CaCu}_3\text{Ti}_4\text{O}_{12} - x\text{MgTiO}_3$ samples at room temperature.

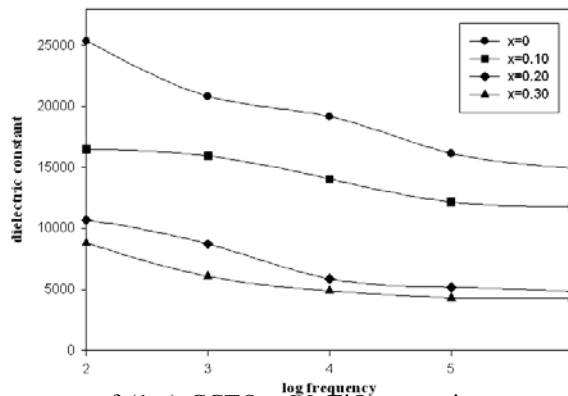


Fig. 5: Plot of dielectric constant of $(1-x)$ CCTO- x MgTiO_3 ceramics versus log of frequency for $x=0-0.3$ at room temperature.

lower frequencies and the decrease in dielectric constant as frequency increases suggests that the dipole does not have sufficient time to respond to the field reversal which takes place over a very short interval of time (Li *et al.*, 2005; Ni *et al.*, 2006; Sabar *et al.*, 2007) Hence, it contributes to a reduction in the dielectric constant. However, the dielectric constants for $x=0.10$, 0.20, 0.30 samples dropped from 17,015 (at 10^2 Hz) to 11,744 (at 10^6 Hz), 10,198 (at 10^2 Hz) to 4,518 (at 10^6 Hz), and 8101 (at 10^2 Hz) to 4,020 (at 10^6 Hz), respectively. Generally, at a particular frequency the relative drop was less as the contents of MgTiO_3 increased. This would suggest that the dielectric constants of the doped samples are almost frequency independent compared to the undoped $x=0$ sample. The frequencies independence could be due to the effect of increasing grain boundary resistance due to the reduction of grain size (Li *et al.*, 2005; Ni *et al.*, 2006).

Higher frequencies would have caused further drop in dielectric constant, but the smaller grain size reduced the impact of intra-well hopping and the inability to sense the field reversal to a minimum. Hence the values of dielectric constant became almost frequency independent.

The frequency dependence of the dielectric loss of MgTiO₃-doped CCTO samples $x= 0-0.3$ measured at room temperature is plotted in Figure 6. At the lowest frequency (10² Hz), the increased addition of MgTiO₃ into CCTO resulted in increasing dielectric loss from 0.201 ($x=0$) to 0.244 ($x=0.3$). However, beyond 10³ Hz, the dielectric loss of all MgTiO₃-doped CCTO samples began to drop below 0.1 for 10⁴ Hz to 10⁶ Hz whereby the lowest value of dielectric loss obtained was 0.05 (at 10⁵ Hz) for the $x=0.3$ sample. The latter is approximately 2 fold (0.0801(for $x=0$)/0.0443(for $x=0.3$)) reduction compared to the undoped $x=0$ sample at the same frequency (10⁵ Hz). According to IBLC model, dielectric loss mainly originates from conductivity of the conducting crystalline grains of CCTO as well as that of the insulating barriers. Based on Table 1, as MgTiO₃ addition to CCTO increased, the grain boundary resistivity also increases and the reduction in conductivity of the barriers narrowed leakage loss (Kwon *et al.*, 2007; Chun Li *et al.*, 2009; Amaral *et al.*, 2010) is possible that insulating MgTiO₃ resides between CCTO grains, causing the inter grains conductivity to decrease. SEM micrographs (Figure 2) also suggest that addition of MgTiO₃ caused reduction in grains size and subsequent increase in density of grains boundary in the samples. The latter contribute to the significant drop in dielectric loss of the doped samples.

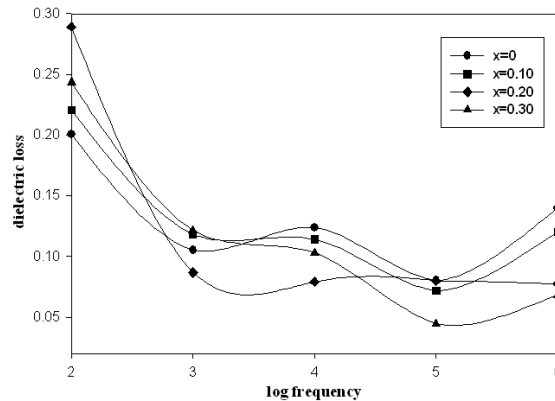


Fig. 6: Plot of dielectric loss of $(1-x) \text{CaCu}_3\text{Ti}_4\text{O}_{12} - x\text{MgTiO}_3$ for $x= 0-0.3$ versus log of frequency at room temperature.

The temperature dependence of dielectric constant for all samples at different frequencies is presented in Fig.7. Generally, at a particular frequency the dielectric constant was observed to increase with temperature for temperatures higher than room temperature. This is probably due to increase in charge carrier mobility at higher temperatures which increases the ability of the charges to align themselves with the applied field in a shorter time when the field changes direction and hence resulted in the increase of the dielectric property. Similar observation was also reported for $\text{CaCu}_3\text{Ti}_{4-x}\text{Zr}_x\text{O}_{12}$ (Om Prakash *et al.*, 2008). Our analysis of the conductivity data shows that it follows the Arrhenius law described by the following expression (Mandal *et al.*, 2009; Sayer *et al.*):

$$\sigma = \sigma_0 \exp (-E_a / kT) \tag{6}$$

where σ is the conductivity, E_a is the activation energy for electron hopping and k is the Boltzmann constant. The values of activation energies were obtained from the least square fitting of the conductivity data. As shown in Fig. 8(a), the slopes of the Arrhenius plot for the grain boundary conductivity shows linear regions, in the range of 300–413K that was used to calculate activation energies at the grains boundary using equation (6) and the results are tabulated in Table 2. Similar plots (Fig. 8(b)) and calculations (Table 2) were also done for grain conductivity data to obtain grain activation energy. Our results in Table 2 indicate that for the same temperature range, the activation energy of the grain boundaries is approximately 2.5 times higher as compared to the activation energy of the grains. The low activation energy for the bulk conductivity process in the range of 0.093-0.096 eV (Table 2) is suited to semiconducting behavior of the grains, while the grain boundary

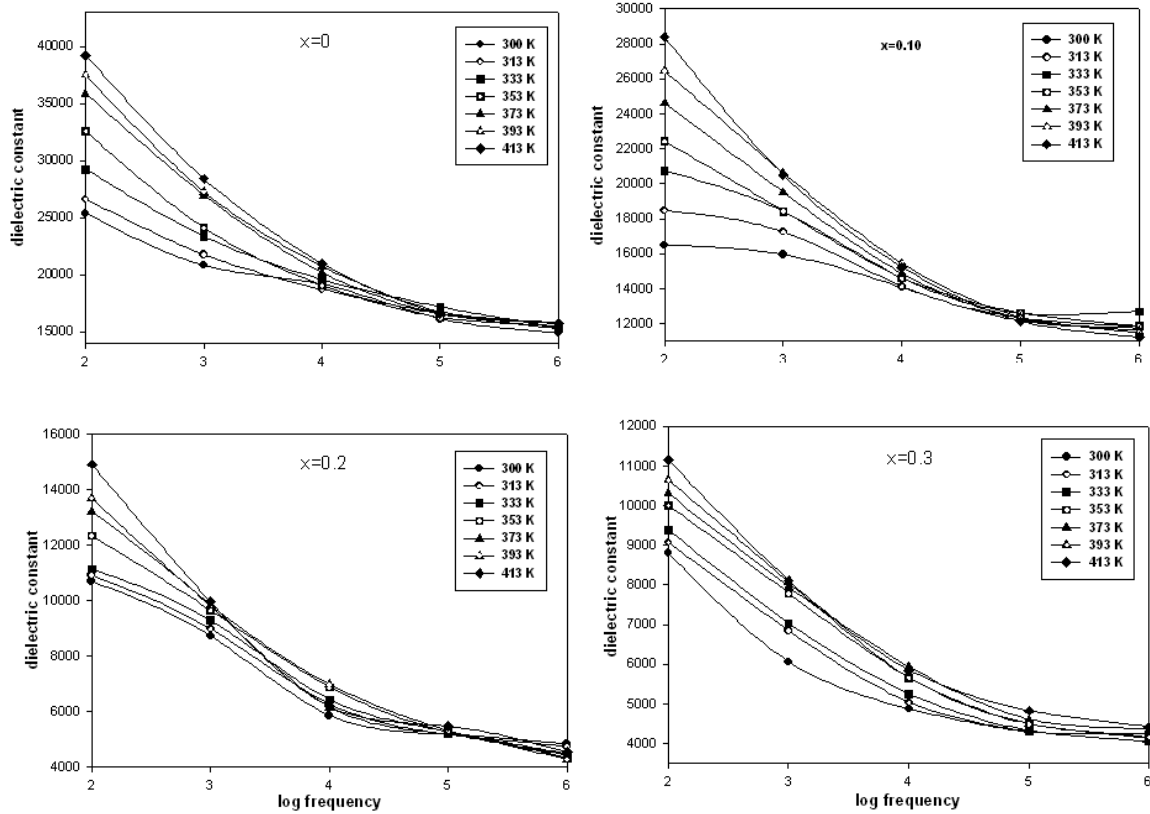


Fig. 7: Frequency dependence of dielectric constant of $(1-x) \text{CaCu}_3\text{Ti}_4\text{O}_{12} - x\text{MgTiO}_3$ at different temperatures for (a) $x=0$ (b) $x= 0.10$ (c) $x= 0.20$ (d) $x=0.30$

Table 2: Activation energy of grain, E_{gb} and gain boundary, E_g in the temperature range of 300-413K

Samples (x)	Activation energy of grain boundary, E_{gb} (eV)	Activation of grain, E_g (eV)
0	0.093	0.204
0.1	0.094	0.207
0.2	0.095	0.208
0.3	0.096	0.211

activation energy was estimated in the range of 0.204-0.211 eV (Table 2), in good agreement with the value reported for $\text{Ca}_{1-x}\text{La}_x\text{Cu}_3\text{Ti}_{4-x}\text{Co}_x\text{O}_{12}$ (Mandal *et al.*, 2009). Existence of activation energies in the conduction mechanism suggests that conductivity at both the grains and the grains boundaries is due to hopping of charge carriers from one site to the other but much larger energy is required to activate the charge carriers at the grains boundaries causing it to be insulating (Sung *et al.*, 2005; Sayer *et al.*, ;Kumar *et al.*, 2007). Our results conform to the IBLC model where grains are electrically semiconducting while grains boundaries are insulating. The results (Table 2) also show that while both activation energies of grain and grain boundaries increased with increasing MgTiO_3 content, the increase in activation energy of the latter is very much larger. It can be effectively suggested that the doping mainly modified the grains boundary regions, probably increasing the potential barriers at the grains boundaries which resulted in large grains boundary resistance, R_{gb} compared to grains resistance, R_g (Table 1) (Sayer *et al.*,).

Ultrasonic velocity measurements showed increasing longitudinal velocity and shear velocity with the addition of MgTiO_3 . Table 4 gives the values of density (ρ), ultrasonic longitudinal velocity (v_L), shear velocity (v_S), longitudinal modulus (C_L), shear modulus (μ), bulk modulus (B) and Young's modulus (Y) of the samples. Each elastic modulus was calculated using formulas given in ref (Rasih and Yahya, 2009). Interestingly, compared to $x=0$ the changes in longitudinal modulus (43.6%) is greater compared to the changes in shear modulus (13.3%) at $x=0.3$. The percentage change in shear velocity increases from 0.50% ($x=0.1$) to 14.43% ($x=0.3$). Similarly, the change in longitudinal velocity also increases from 11.31% ($x=0.1$) to 28.83% ($x=0.3$). Fig. 10 shows increasing C_L with MgTiO_3 addition from $x=0.0$ (32.5 GPa) to $x=0.3$ (50.9 GPa). This increasing

Table 3: Values of density (ρ), longitudinal velocity (v_L), shear velocity (v_s), longitudinal modulus (C_L), shear modulus (μ), bulk modulus (B), Young's modulus (Y) of the $x=0.0, 0.2, 0.3$ samples at room temperature. The values were corrected for porosity.

Samples (x)	Porosity(%)	$v_L(\text{kms}^{-1})$	$v_s(\text{kms}^{-1})$	$C_L(\text{Gpa})$	$\mu(\text{GPa})$	$B(\text{GPa})$	$Y(\text{GPa})$
0	10.5	2.90(1)	2.12(1)	40.6(3)	21.8(2)	11.5(3)	40(2)
0.1	10.4	3.22(1)	2.13(2)	49.9(2)	21.9(1)	20.7(2)	48(1)
0.2	7.6	3.32(2)	2.18(2)	51.0(1)	22.2(3)	21.5(4)	49(3)
0.3	6.4	3.65(1)	2.38(2)	58.2(4)	24.7(3)	25.3(2)	56(4)

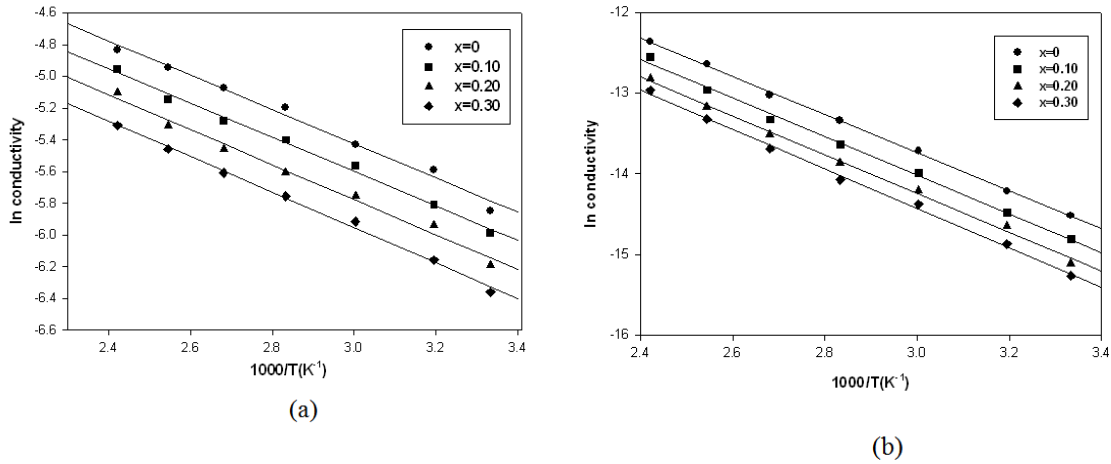


Fig. 8: Plot of (a) $\ln \sigma$ of grain boundary versus $1000/T$ (K^{-1}) and (b) $\ln \sigma$ of grains versus $1000/T$ (K^{-1}) for $(1-x) \text{CaCu}_3\text{Ti}_4\text{O}_{12}-x\text{MgTiO}_3$ ($x= 0-0.3$) samples.

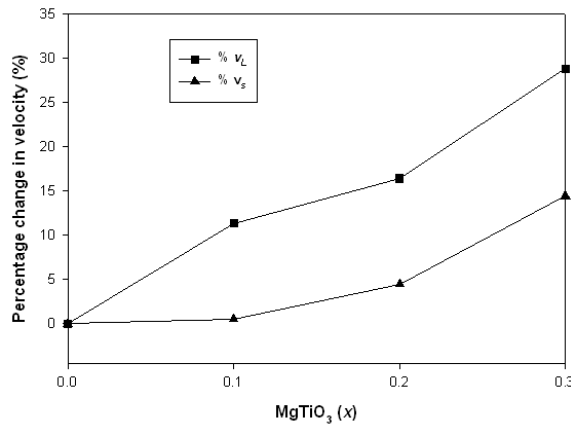


Fig. 9: Percentage change in longitudinal velocity (v_L) and shear velocity (v_s) with MgTiO_3 content for $(1-x) \text{CaCu}_3\text{Ti}_4\text{O}_{12} - x\text{MgTiO}_3$ sample at room temperature.

trend with MgTiO_3 addition is repeated for the shear modulus (μ) from $x=0.0$ (17.5 GPa) to $x=0.3$ (21.7 GPa). Furthermore, at $x=0.3$, the Young's modulus (Y) (Fig.11) increased by more than 16 GPa compared to undoped CCTO($x=0$). Bulk modulus (B) (Fig.11) also shows an increase from 11.5 GPa ($x=0$) to 25.3 GPa ($x=0.3$). The increase of v_s and v_L with the addition of MgTiO_3 (Fig 9) can be understood from the behavior of the independent moduli (longitudinal modulus, C_L and shear modulus, μ) in concurrence with the variation of density (ρ) as $v_s^2 = \mu/\rho$ and $v_L^2 = C_L/\rho$ (Mallawany, 1998). Hence, the increase in both v_s and v_L is related to the decrease in density, ρ . However, the influence of density on velocity is limited with the density change of not more than 10%. Instead, the increase in both v_s and v_L is suggested to be also influenced by the increase in longitudinal modulus, C_L (43.6%) and shear modulus, μ (13.3%). It is suggested that MgTiO_3 resides at the grain boundary and contributed to inter-grain strengthening effect which improves the elastic moduli.

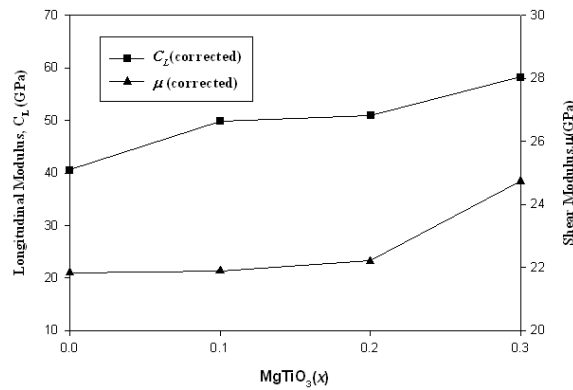


Fig. 10: Longitudinal modulus (C_L) and shear modulus (μ) versus $MgTiO_3$ content for $(1-x) CaCu_3Ti_4O_{12} - xMgTiO_3$ sample at room temperature. (Corrected)

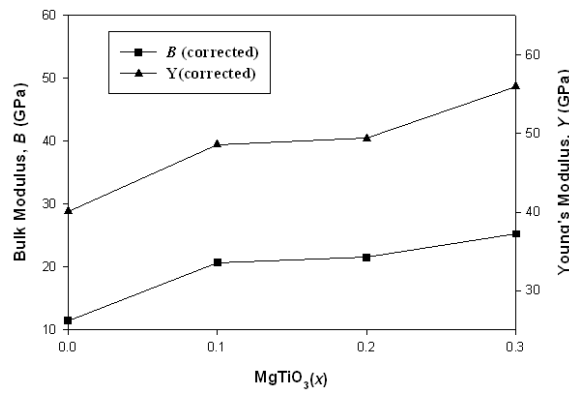


Fig. 11: Bulk modulus (B) and Young's modulus (Y) versus $MgTiO_3$ for $(1-x) CaCu_3Ti_4O_{12} - xMgTiO_3$ sample at room temperature. (Corrected)

Conclusion:

Ceramic composite samples with starting composition of $(1-x) CaCu_3Ti_4O_{12} - xMgTiO_3$ were successfully prepared by solid state synthesis method to study the effects of $MgTiO_3$ doping on dielectric properties of CCTO. Addition of $MgTiO_3$ caused reduction of dielectric constant but reasonable values of the dielectric constant in the range of $1.7-1.1 \times 10^4$ was obtained at $x=0.1$ besides significantly improved stability with frequency compared to the undoped $x=0$ sample. The addition of $MgTiO_3$ also effectively reduced the dielectric loss of all doped samples with the $x=0.3$ sample recording a loss of well below 0.05 (at 10^4 Hz). The reduction in dielectric loss is suggested to be due to $MgTiO_3$ residing at the grains boundaries causing enhancement in grains boundary resistivity which in turn impedes charge leakage as the $MgTiO_3$ content increased. Activation energy obtained from Arrhenius plots of log of conductivity, $\ln s$ versus $1000/T$ showed considerable increase in grains-boundary activation energy, E_{gb} with increasing $MgTiO_3$ content which explains the increasing insulative character of the grains boundary compared to the semiconducting grains. Ultrasonic velocity measurements showed $MgTiO_3$ addition significantly improves elastic properties of CCTO.

ACKNOWLEDGMENTS

This research has been supported by the Malaysian Ministry of Higher Education under Fundamental Research Grant Scheme.

REFERENCES

Amaral, F., M.A. Valente, L.C. Costa, 2010. 'Dielectric properties of $CaCu_3Ti_4O_{12}$ (CCTO) doped with GeO_2 ', *Journal of Non-Crystalline Solids*, 356: 822-827.

Almeida, A.F.L., P.B.A. Fechine, J.C. Góes, M.A. Valente, M.A.R. Miranda, A.S.B. Sombra, 2004. 'Dielectric properties of BaTiO₃ (BTO)–CaCu₃Ti₄O₁₂ (CCTO) composite screen-printed thick films for high dielectric constant devices in the medium frequency (MF) range', *Materials Science and Engineering B*, 111: 113-123.

Adams, T.B., D.C. Sinclair, A.R. West, 2002. 'Giant barrier layer capacitance effects in CaCu₃Ti₄O₁₂ ceramics', *Advanced Materials*, 14: 18.

Capsoni, D., M. Bini, V. Massarotti, G. Chioldelli, 2004. 'Role of doping and CuO segregation in improving the giant permittivity of CaCu₃Ti₄O₁₂', *Journal of Solid State*, 177: 4494-4500.

Chun Hong Mu, Peng Liu, Ying He, Jian Ping Zhou, Huai Wu Zhang, 2009. 'An effective method to decrease dielectric loss of CaCu₃Ti₄O₁₂ ceramics', *Journal of Alloys and Compound*, 417: 137-141.

Chih Ming Wang, Shih Yuan Lin, Kuo Sheng Kao, Ying Chung Chen and Shang Chih Weng, 2010. 'Microstructural and electrical properties of CaTiO₃-CaCu₃Ti₄O₁₂ ceramics', *Journal of Alloys and Compounds*, 491: 423-430.

Chioldelli, G., V. Massarotti, D. Capsoni, M. Bini, C.B. Azzoni, M.C. Mozzati, P. Lupotto, 2004. 'Electric and dielectric properties of pure and doped CaCu₃Ti₄O₁₂ perovskite materials', *Solid State Communications*, 132: 241-246.

Feng, L., X. Tang, Y. Yan, X. Chen, Z. Jiao, G. Cao, 2006. 'Decrease of dielectric loss in CaCu₃Ti₄O₁₂ ceramics by La doping', *Physica Status Solidi*, 203(4): 22-24.

Guozhong Zang, Jialiang Zhang, Peng Zheng, Jinfeng and Chunlei Wang, 2005. 'Grain boundary effect on the dielectric properties of CaCu₃Ti₄O₁₂ ceramics', *Journal of Physics D: Applied Physics*, 38: 1824-1827.

Hongtao Yu, Hanxing Liu, Hua Hao, Dabing Lu, Minghe Cao, 2008. 'Dielectric properties of CaCu₃Ti₄O₁₂ ceramics modified by SrTiO₃', *Materials Letters*, 62: 1353-1355.

Kang-Min Kim, Sun-Jung Kim, Jong-Heun Lee, Doh-Yeon Kim, 2007. 'Microstructural evolution and dielectric properties of SiO₂-doped CaCu₃Ti₄O₁₂ ceramics', *Journal of the European Ceramic Society*, 27: 3991-3995.

Li, J., A.W. Sleight, M.A. Subramanian, 2005. 'Evidence for internal resistive barriers in a crystal of the giant dielectric constant material: CaCu₃Ti₄O₁₂', *Solid State Communications*, 135: 260-262.

Lin, T.N., J.P. Chu, S.F. Wang, 2005. 'Structures and properties of Ba_{0.3}Sr_{0.7}TiO₃:MgTiO₃ ceramic composites', *Materials Letters*, 59: 2786-2789.

Mallawany, R. El-, 1998. 'Tellurite glasses', *Materials Chemistry and Physics*, 53: 93-120.

Mandal, K.D., Alok Kumar Rai, D. Kumar and Om Prakash, 2009. 'Dielectric properties of the Ca_{1-x}La_xCu₃Ti_{4-x}Co_xO₁₂ system (x = 0.10, 0.20 and 0.30) synthesized by Semi-wet Route', *Journal of Alloys and Compounds*, 478: 771-776.

Mazni Mustafa, W. Mohamad Daud W. Yusoff, Zainal Abidin Talib, Abdul Halim Shaari and Walter Charles Primus, 2009. 'Impedance studies on Ca_{0.5}Sr_{0.5}Cu₃Ti₄O₁₂ ceramic Oxide', *Pertanika J. Science & Technology*, 17: 131-136.

Majid, S.R., A.K. Arof, 2007. 'Electrical behavior of proton-conducting chitosan-phosphoric acid-based electrolytes', *Physica B*, 390: 209-215.

Marques, V.P.B., A. Ries, A.Z. Simões, M.A. Ramírez, J.A. Varela, E. Longo, 2007. 'Evolution of CaCu₃Ti₄O₁₂ varistor properties during heat treatment in vacuum', *Ceramics International*, 33: 1187-1190.

Muhammad Azwadi Sulaiman, Sabar D. Hutagalunga, Mohd Fadzil Ainb, Zainal A. Ahmad, 2010. 'Dielectric properties of Nb-doped CaCu₃Ti₄O₁₂ electroceramics measured at high frequencies', *Journal of Alloys and Compounds*, 49: 486-492.

Ni, L., X.M. Chen, X.Q. Liu, R.Z. Hou, 2006. 'Microstructure-dependent giant dielectric response in CaCu₃Ti₄O₁₂ ceramics', *Solid State Communications*, 139: 45-50.

Om Parkash, Devendra Kumar, Anubha Goyal, Anupriya, Ankita Mukhejee, Sindhu Singh and Prakash Singh, 2008. 'Electrical behaviour of zirconium doped calcium copper titanium oxide', *Journal of Physics*, 4: 035401(8pp).

Pradip Kumar Jana, Sudipta Sarkar and B.K. Chaudhuri, 2007. 'Maxwell–Wagner polarization mechanism in potassium and titanium doped nickel oxide showing giant dielectric permittivity', *J.Phys. D: Appl. Phys.*, 40: 556-560.

Peng Liu, Jianli Ma, Ling Meng, Jun Li, Jingliang Wang, 2009. 'Preparation and dielectric properties of BST-Mg₂TiO₄ composite ceramics', *Materials Chemistry and Physics*, 114: 624-628.

Ramirez, A.P., M.A. Subramanian, M. Gardel, G. Blumberg, D. Li, T. Vogt, S.M. Shapiro, 2000. 'Giant dielectric constant response in a copper-titanate', *Solid State Communications*, 115: 217-200.

Rasih, N.A., A.K. Yahya, 2009. 'Effect of Ba-site substitution by Sr on ultrasonic velocity and electron-phonon coupling constant of $\text{DyBa}_{2-x}\text{Sr}_x\text{Cu}_3\text{O}_{7-d}$ superconductors', *Journal of Alloys and Compounds*, 480: 777- 781.

Sabar D.Hutagalung, Ooi Li Ying and Zainal Arifin Ahmad, 2007. 'Effect of sintering temperature on the properties of modified mechanical alloyed $\text{CaCu}_3\text{Ti}_4\text{O}_{12}$ ', *IEEE Transactions on ultrasonics, Ferroelectrics and Frequency contro*, 154: 12.

Sabar D. Hutagalung, Li Ying Ooi, Zainal A. Ahmad, 2009. 'Improvement in dielectric properties of Zn-doped $\text{CaCu}_3\text{Ti}_4\text{O}_{12}$ electroceramics prepared by modified mechanical alloying technique', *Journal of Alloys and Compounds*, 476: 477-481.

Sayer, M., A. Mansingh, J.B. Webb and J. Noad, 1978. 'Long-range potential centres in disordered solids', *Journal of Physics C: Solid State Phys.*, 11: 315.

Subramanian, M.A., A.W. Sleight, 2002. ' $\text{ACu}_3\text{Ti}_4\text{O}_{12}$ and $\text{ACu}_3\text{Ru}_4\text{O}_{12}$ perovskites: high dielectric constants and valence degeneracy', *Solid State Sciences*, 4: 347-351.

Subramanian, M.A., Dong Li, N. Duan, B.A. Reisner and A.W. Sleight, 2000. 'High dielectric constant in $\text{ACu}_3\text{Ti}_4\text{O}_{12}$ and $\text{ACu}_3\text{Ti}_3\text{FeO}_{12}$ phases', *Solid State Chemistry*, 151: 323-325.

Seunghwa Kwon, Chien-Chih Huang, Eric A. Patterson, David P.Cann, David, P.Cann, 2008. 'The effect of Cr_2O_3 , Nb_2O_5 and ZrO_2 doping on the dielectric properties of $\text{CaCu}_3\text{Ti}_4\text{O}_{12}$ ', *Materials Letters*, 62: 633-636.

Sung Dong Cho, Sang Yong Lee, Jin Gul Hyun, Kyung Wook Paik, 2005. 'Comparison of the theoretical predictions and experimental values of the dielectric constant of epoxy/ BaTiO_3 composite embedded capacitor films', *Journal of Materials in Electronic*, 16: 77-84.

Yi-Cheng Liou, Wen-Chou Tsai, Song-Ling Yang. 'Synthesis of 0.95MgTiO_3 - 0.05CaTiO_3 ceramics by reaction-sintering', In the proceedings of the 16th International conference on composite materials.

Yueyue Yan, Lei Jin, Lixin Feng, Guanghan Cao, 2006. 'Decrease of dielectric loss in giant dielectric constant $\text{CaCu}_3\text{Ti}_4\text{O}_{12}$ ceramics by adding CaTiO_3 ', *Materials Science and Engineering*, 130: 146-150.